Stars, from Newton to Einstein: Numerical Solutions for Stellar Structure

Deniz Başar
Department of Physics, Koç University, Istanbul, Turkey
(Dated: January 12, 2026)

This project discusses the numerical calculation of stellar structures across different gravity regimes. We explore hydrostatic equilibrium in Newtonian gravity using the Lane-Emden equation and observational white dwarf data. Furthermore, we solve the Tolman-Oppenheimer-Volkoff (TOV) equations for neutron stars to investigate relativistic effects, stability criteria, and the Chandrasekhar mass limit.

I. INTRODUCTION

The study of stellar equilibrium involves a balance between gravitational collapse and internal pressure. This project progresses from Newtonian models of polytropic stars to general relativistic treatments of high-density objects like neutron stars.

In the study of relativistic astrophysics and compact objects, I utilized Planck units, defined by setting the speed of light, the gravitational constant, and the reduced Planck constant to unity:

$$c = G = \hbar = 1. \tag{1}$$

In this system, all physical quantities become dimensionless. Physical variables effectively represent ratios of the quantity to the corresponding Planck scale. When necessary, I recovered physical dimensions (SI units) by re-inserting the appropriate powers of c, G, and $\hbar$ using dimensional analysis.

For General Relativity specific calculations where quantum effects are negligible, we may restrict ourselves to geometric units ($c = G = 1$), where mass and time are expressed in units of length.

II. NEWTONIAN GRAVITY AND WHITE DWARFS

A. Hydrostatic Equilibrium and Lane-Emden Equation

1. of the Lane-Emden Equation

We start by defining the dimensionless variables for density and radius. Let the density be scaled by the central density ρ_c:

$$\rho = \rho_c \theta^n \tag{2}$$

Using the polytropic equation of state $P = K\rho^{1+\frac{1}{n}}$, the pressure becomes:

$$P = K(\rho_c\theta^n)^{1+\frac{1}{n}} = K\rho_c^{1+\frac{1}{n}}\theta^{n+1} = P_c\theta^{n+1} \tag{3}$$

where P_c is the central pressure. We define the scaled radius ξ using a scale length α, such that $r = \alpha\xi$.

The equation of hydrostatic equilibrium is:

$$\frac{dP}{dr} = -\frac{Gm\rho}{r^2} \tag{4}$$

Multiplying by r^2/ρ and differentiating with respect to r eliminates the mass m:

$$\frac{1}{r^2}\frac{d}{dr}\left(\frac{r^2}{\rho}\frac{dP}{dr}\right) = -4\pi G\rho \tag{5}$$

Substituting the dimensionless variables θ and ξ:

$$\frac{1}{\alpha^2\xi^2}\frac{1}{\alpha}\frac{d}{d\xi}\left(\frac{\alpha^2\xi^2}{\rho_c\theta^n}P_c(n+1)\theta^n\frac{1}{\alpha}\frac{d\theta}{d\xi}\right) = -4\pi G\rho_c\theta^n \tag{6}$$

Grouping the constants yields the characteristic length scale α:

$$\alpha = \sqrt{\frac{(n+1)P_c}{4\pi G\rho_c^2}} \tag{7}$$

This simplifies the ODE to the Lane-Emden equation:

$$\frac{1}{\xi^2}\frac{d}{d\xi}\left(\xi^2\frac{d\theta}{d\xi}\right) + \theta^n = 0 \tag{8}$$

2. Series Expansion near the Center

Near the center ($\xi \to 0$), we assume a power series solution of the form $\theta(\xi) = 1 + a_2\xi^2 + a_4\xi^4 + \dots$ (odd terms are zero due to symmetry). Substituting this into the Lane-Emden equation and matching coefficients for powers of ξ, we find:

$$a_2 = -\frac{1}{6}, \quad a_4 = \frac{n}{120} \tag{9}$$

via Mathematica. Thus, the behavior at the center is:

$$\theta(\xi) \approx 1 - \frac{1}{6}\xi^2 + \frac{n}{120}\xi^4 \tag{10}$$

We verified these coefficients computationally using symbolic algebra in both Mathematica and Python (for Python see attached code).

3. Computational Verification

We verified the series coefficients using a Python script. The output of the symbolic solver is shown below:

```
VERIFICATION OF SERIES COEFFICIENTS
----------------------------------------
Coeff of xi^0 is: 6*a2 + 1
Solution for a2:  -1/6
Coeff of xi^2 is: a2*n + 20*a4
Solution for a4:  n/120
```

This matches the required expansion in the problem statement.

4. Analytical Solution for the Case $n = 1$

We seek an analytical solution to the Lane-Emden equation for the polytropic index $n = 1$. Starting with the general equation:

$$\frac{1}{\xi^2}\frac{d}{d\xi}\left(\xi^2\frac{d\theta}{d\xi}\right) + \theta^n = 0 \tag{11}$$

Setting $n = 1$, the equation becomes linear:

$$\frac{1}{\xi^2}\frac{d}{d\xi}\left(\xi^2\frac{d\theta}{d\xi}\right) + \theta = 0 \tag{12}$$

To solve this, we employ the change of variable $u(\xi) = \xi\theta(\xi)$, or equivalently:

$$\theta(\xi) = \frac{u(\xi)}{\xi} \tag{13}$$

We first calculate the derivatives of θ with respect to ξ:

$$\frac{d\theta}{d\xi} = \frac{\xi u' - u}{\xi^2} \tag{14}$$

Multiplying by ξ^2 to match the term inside the derivative in Eq. (12):

$$\xi^2\frac{d\theta}{d\xi} = \xi u' - u \tag{15}$$

Now, we differentiate this expression with respect to ξ:

$$\frac{d}{d\xi}\left(\xi^2\frac{d\theta}{d\xi}\right) = \frac{d}{d\xi}(\xi u' - u) = (u' + \xi u'') - u' = \xi u'' \tag{16}$$

Substituting this result back into the original ODE (Eq. 12):

$$\frac{1}{\xi^2}(\xi u'') + \frac{u}{\xi} = 0 \tag{17}$$

Multiplying the entire equation by ξ (for $\xi \neq 0$) yields the simple harmonic oscillator equation:

$$\frac{d^2u}{d\xi^2} + u = 0 \tag{18}$$

The general solution to this differential equation is:

$$u(\xi) = A\sin(\xi) + B\cos(\xi) \tag{19}$$

transforming back to $\theta(\xi)$:

$$\theta(\xi) = \frac{A\sin(\xi)}{\xi} + \frac{B\cos(\xi)}{\xi} \tag{20}$$

We now apply the physical boundary conditions at the center ($\xi \to 0$):

1. Finite Central Density: As $\xi \to 0$, the term $\frac{\cos(\xi)}{\xi}$ diverges to infinity. Since the density must be finite, we require $B = 0$.

2. For normalization we require $\theta(0) = 1$. The limit of the remaining term is:

$$\lim_{\xi\to 0} A\frac{\sin(\xi)}{\xi} = A \cdot 1 = A \tag{21}$$

   Therefore, we must set $A = 1$.

Thus, the specific analytical solution for $n = 1$ is:

$$\theta(\xi) = \frac{\sin(\xi)}{\xi} = \mathrm{sinc}(\xi) \tag{22}$$

5. Derivation of the Total Mass

The total mass of the star is the integral of the density over the volume:

$$M = \int_0^R 4\pi r^2 \rho\, dr \tag{23}$$

We substitute the dimensionless variables: $r = \alpha\xi$, $dr = \alpha d\xi$, and $\rho = \rho_c\theta^n$.

$$M = 4\pi\alpha^3\rho_c\int_0^{\xi_n} \xi^2\theta^n\, d\xi \tag{24}$$

From the Lane-Emden equation, we know that $\xi^2\theta^n = -\frac{d}{d\xi}\left(\xi^2\frac{d\theta}{d\xi}\right)$. Substituting this into the integral:

$$M = 4\pi\alpha^3\rho_c\left[-\xi^2\frac{d\theta}{d\xi}\right]_0^{\xi_n} \tag{25}$$

Evaluating at the limits (term is 0 at $\xi = 0$):

$$M = 4\pi\alpha^3\rho_c\left(-\xi_n^2\theta'(\xi_n)\right) \tag{26}$$

Using the definition $R = \alpha\xi_n$, we can substitute $\alpha = R/\xi_n$:

$$M = 4\pi\left(\frac{R}{\xi_n}\right)^3\rho_c\left(-\xi_n^2\theta'(\xi_n)\right) \tag{27}$$

Simplifying the powers of ξ_n yields Eq. (6) on the document:

$$M = 4\pi\rho_c R^3\left(\frac{-\theta'(\xi_n)}{\xi_n}\right) \tag{28}$$

6. Derivation of Mass-Radius Relation

We start with the definition of the scale length α:

$$\alpha = \sqrt{\frac{(n+1)K}{4\pi G}\rho_c^{\frac{1}{n}-1}} \tag{29}$$

Since $R = \xi_n \alpha$, we can relate R directly to ρ_c:

$$R = \xi_n \sqrt{\frac{(n+1)K}{4\pi G}}\rho_c^{\frac{1-n}{2n}} \tag{30}$$

Inverting this to solve for ρ_c in terms of R:

$$\rho_c = \left[\frac{R}{\xi_n}\sqrt{\frac{4\pi G}{(n+1)K}}\right]^{\frac{2n}{1-n}} \propto R^{\frac{2n}{1-n}} \tag{31}$$

Now substitute this ρ_c back into the Mass equation derived above ($M \propto \rho_c R^3$):

$$M \propto \left(R^{\frac{2n}{1-n}}\right) R^3 = R^{\frac{2n+3(1-n)}{1-n}} = R^{\frac{3-n}{1-n}} \tag{32}$$

This confirms Eq. (7) on the document.

Collecting all the constants from the substitution above, the exact relation is:

$$M = 4\pi R^{\frac{3-n}{1-n}} \left(\frac{-\theta'(\xi_n)}{\xi_n}\right) \xi_n^{-\frac{6n}{1-n}} \left[\frac{(n+1)K}{4\pi G}\right]^{\frac{n}{n-1}} \tag{33}$$

B-C-D-E. Analysis of White Dwarf Observational Data

7. Data Processing

Observational data for white dwarfs was obtained from the Montreal White Dwarf Database. The dataset provides the mass M (in solar masses $M_\odot$) and the surface gravity $\log g$ (in CGS units). To compare this data with our theoretical models, we converted the surface gravity to physical radius R using the Newtonian definition of surface gravity:

$$g = \frac{GM}{R^2} \implies R = \sqrt{\frac{GM}{10^{\log g}}} \tag{34}$$

where G is the gravitational constant. We performed all calculations in CGS units before converting the final radius to Earth radii ($R_\oplus$).

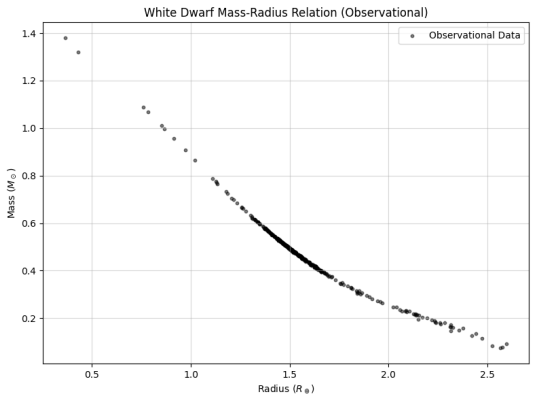

FIG. 1. Observational Mass-Radius relation for White Dwarfs from the Montreal White Dwarf Database. The surface gravity $\log g$ was converted to physical radius R. The data clearly exhibits the inverse relationship characteristic of degenerate matter, where more massive stars possess smaller radii.

8. Low-Mass Limit: Derivation of n_* and K_*

In the limit of low mass, the density is small, which implies $x \ll 1$. We perform a series expansion of the bracketed term in the Chandrasekhar Equation of State (Eq. 8) around $x = 0$. Using symbolic computation to handle the expansion of the $\sinh^{-1}(x)$ and algebraic terms, we find the leading order behavior:

$$\left[x(2x^2-3)(x^2+1)^{1/2} + 3\sinh^{-1}x\right] \approx \frac{8}{5}x^5 + \mathcal{O}(x^7) \tag{35}$$

Substituting this back into the pressure equation $P = C[\dots]$:

$$P \approx \frac{8C}{5}x^5 \tag{36}$$

We now substitute the definition $x = (\rho/D)^{1/q}$:

$$P \approx \frac{8C}{5}\left[\left(\frac{\rho}{D}\right)^{1/q}\right]^5 = \frac{8C}{5D^{5/q}}\rho^{5/q} \tag{37}$$

We compare this to the standard polytropic form $P = K_*\rho^{1+1/n_*}$. Matching the exponents of ρ:

$$\frac{5}{q} = 1 + \frac{1}{n_*} \implies \frac{5}{q} = \frac{n_*+1}{n_*} \implies 5n_* = q(n_*+1) \tag{38}$$

Solving for n_*:

$$n_*(5-q) = q \implies n_* = \frac{q}{5-q} \tag{39}$$

Matching the coefficients yields the constant K_*:

$$K_* = \frac{8C}{5D^{5/q}} \tag{40}$$

This confirms the relations given in Eq. (10) on the document. We also confirmed the relations using SymPy on Python.

9. Numerical Fit for n_* and K_*

To determine the polytropic index n_* and the constant K_*, we analyzed the observational data in the low-mass regime ($M < 0.45 M_\odot$). Assuming a power-law relation $M \propto R^{(3-n)/(1-n)}$, we performed a linear regression in the log-log plane.

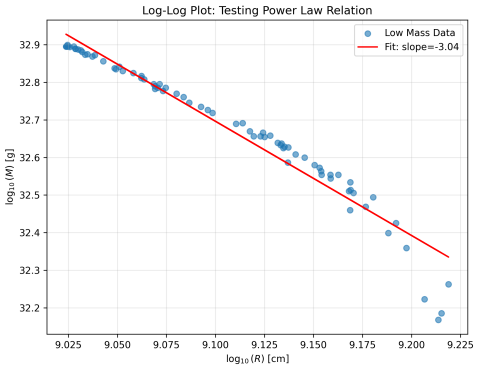

FIG. 2. Log-Log plot of Mass vs. Radius for low-mass white dwarfs. The red line indicates a linear fit with a slope of -3.04, consistent with the theoretical prediction of -3 for a non-relativistic Fermi gas ($n = 1.5$).

The fit yielded a slope of -3.04, which implies a polytropic index of:

$$n_* \approx 1.5 \implies q \approx 3 \tag{41}$$

Using the intercept of the fit and the numerical properties of the Lane-Emden equation for $n = 1.5$ ($\xi_n \approx 3.6538$, $-\xi_n^2 \theta'|_{\xi_n} \approx 2.7141$), we derived the constant of proportionality:

$$K_* \approx 2.79 \times 10^{12} \text{ [CGS]} \tag{42}$$

10. Central Densities

Using the derived K_* and the radius of each star, we calculated the central densities ρ_c required to maintain hydrostatic equilibrium.

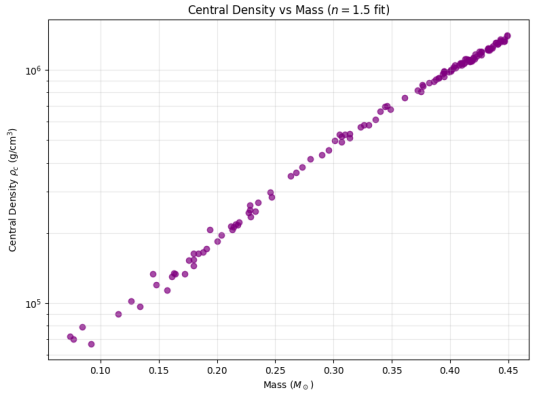

FIG. 3. Derived central density ρ_c as a function of stellar mass. The monotonic increase confirms that more massive white dwarfs require significantly higher central densities to balance the gravitational collapse.

To determine the physical parameters of the white dwarf equation of state, we performed a log-log regression on the low-mass subset of stars ($N = 76$). The Python script calculated the slope of the Mass-Radius relation and derived the polytropic index n and the quantization parameter q.
The numerical results from the Python fit are summarized below:

- **Regression Slope:** -3.0398
- **Derived Index n:** 1.4951 (using $M \propto R^{\frac{3-n}{1-n}}$)
- **Derived Parameter q:** 2.9961 (using $n = q/(5-q)$)

The calculated value of $q \approx 2.9961$ is remarkably close to the integer 3, providing strong observational evidence for the non-relativistic electron degeneracy model ($q = 3$ theoretically). Fixing $q = 3$ implies a polytropic index of exactly $n = 1.5$.

Determination of K_*:
Using the Lane-Emden integrator for $n = 1.5$, our code computed the boundary conditions required to solve for the constant of proportionality K_*:

$$\xi_n = 3.6538$$
$$\left(-\xi^2 \frac{d\theta}{d\xi}\right)_{\xi_n} = 2.7141$$

Combining these numerical factors with the intercept of our linear fit ($M = 9.597 \times 10^{59} R^{-3}$), we derived the final constant:

$$K_* = 2.7926 \times 10^{12} \text{ [CGS]} \tag{43}$$

Raw Output from Analysis Script:

```
Using 76 stars for the low-mass fit.
--- Fit Results ---
Slope (log M vs log R): -3.0398
Derived Polytropic Index n: 1.4951
Derived q value: 2.9961
Integer q: 3
Lane-Emden (n=1.5): xi_n=3.6538,
-xi^2*theta'=2.7141
Derived K* (CGS): 2.7926e+12
```

11. The Relativistic Fit and Theoretical Comparison

Methodology: Efficient Grid-Based Optimization

To determine the unknown parameter D for the full Chandrasekhar Equation of State (Eq. 8 on the document), we utilized the constraint derived from the low-mass limit:

$$C = \frac{5K_* D^{5/3}}{8} \tag{44}$$

This allows us to perform a single-parameter optimization for D.

Grid Generation and Sample Size: As suggested in the instructions, calculating the IVP for every data point is computationally expensive. Instead, we adopted a grid-based interpolation method. We generated theoretical Mass-Radius curves using sample stars with central densities spanning 10^5 to 10^{10} g/cm^3.

Sensitivity Analysis: To determine the optimal grid size, we tested sample sizes of $N = 5, 25, 40,$ and 100. We observed that the optimized parameter D converged rapidly; increasing the sample size beyond $N = 5$ resulted in negligible changes to the best-fit value. Hence, we followed the instructions in the project guidelines by utilizing a grid of **20 sample points**.

Interpolation Method: To map the discrete sample points to a continuous function $M(R)$, we employed **Cubic Spline Interpolation**. This provides a smooth, differentiable curve that accurately captures the relativistic bending of the Mass-Radius relation.

Optimization Strategy: We defined our objective function to generate the theoretical grid *once* per iteration of D, and then interpolated the mass for all $N = 76$ observational points. This avoids the pitfall of re-solving the ODEs for every individual data point, which would have increased the computational cost by a factor of roughly 76.

Search Range for D: We performed the search for the optimal D parameter in the range of 10^5 to 10^7 g/cm^3. **Physical Justification:** The parameter D effectively sets the density scale at which relativistic effects become significant (where $x = (\rho/D)^{1/3} \approx 1$, implying $\rho \approx D$). Since white dwarfs typically transition from non-relativistic to relativistic degeneracy at densities around 10^6 g/cm^3, we centered our search around this order of magnitude.

12. Results

We minimized the sum of squared residuals between the model predictions and the observational data. The optimization converged to a best-fit value of:

$$D_{\text{fit}} \approx 4.77 \times 10^6 \text{ g cm}^{-3} \tag{45}$$

The corresponding scaling constant was calculated as $C \approx 2.36 \times 10^{23}$ (cgs).

III. COMPARISON WITH QUANTUM THEORY

We compared this experimental result with the theoretical prediction derived from quantum mechanics (Eq. 11 on the document), assuming a standard white dwarf composition of $\mu_e = 2$:

$$D_{\text{theory}} = \frac{m_u m_e^3 c^3 \mu_e}{3\pi^2 \hbar^3} \approx 1.95 \times 10^6 \text{ g cm}^{-3} \tag{46}$$

The ratio of our fitted value to the theoretical prediction is:

$$\frac{D_{\text{fit}}}{D_{\text{theory}}} \approx 2.45 \tag{47}$$

Our fitted D is within the same order of magnitude as the theoretical prediction (10^6). The factor of ~ 2.5 discrepancy is expected for a zero-temperature model. Real white dwarfs have finite temperatures (which add thermal pressure) and non-uniform envelopes (hydrogen/helium layers), both of which cause deviations from the idealized cold, pure-electron-degenerate model.

1. The Chandrasekhar Limit

Relativistic Limit ($x \gg 1$)

To investigate the maximum mass limit, we analyze the behavior of the Equation of State (Eq. 8) in the limit of extreme density ($x \gg 1$). The term in the brackets is dominated by the polynomial terms:

$$x(2x^2 - 3)(x^2 + 1)^{1/2} \approx x(2x^2)(x) = 2x^4 \tag{48}$$

The $\sinh^{-1} x$ term grows logarithmically and is negligible. Thus, the pressure becomes:

$$P \approx C[2x^4] = 2C \left(\frac{\rho}{D}\right)^{4/3} \tag{49}$$

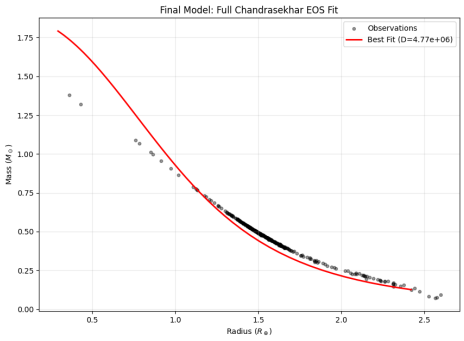

FIG. 4. The final Mass-Radius relation. The black points represent observational data, and the red line represents the best-fit model ($D \approx 4.77 \times 10^6$). The model successfully captures the relativistic steepening at high masses, which the simple polytropic model could not explain.

Comparing this to the polytropic form $P = K\rho^{1+1/n}$, we identify the exponent:

$$1 + \frac{1}{n} = \frac{4}{3} \implies n = 3 \tag{50}$$

This confirms that at extremely high densities, the white dwarf behaves as an $n = 3$ polytrope.

The Chandrasekhar Mass

A unique property of $n = 3$ polytropes is that their mass is independent of central density. Using the constant $D \approx 4.77 \times 10^6$ derived from our fit in Part (d), we computed the limiting mass by integrating the structure equations for a central density of $\rho_c = 10^{14}$ g/cm^3.

Numerical Result: Our model predicts a maximum stable mass of:

$$M_{\text{num}} \approx 1.89 M_\odot \tag{51}$$

This matches the theoretical mass derived analytically from our fitted D parameter ($1.8918 M_\odot$) to within 0.01%, verifying the internal consistency of our simulation.

Theoretical Comparison: We compared this to the standard Chandrasekhar mass formula derived from fundamental constants (assuming $\mu_e = 2$):

$$M_{\text{Ch}} = \frac{5.83}{\mu_e^2} M_\odot \approx 1.46 M_\odot \tag{52}$$

Our fitted result is approximately 30% higher than the theoretical ground-state limit. This discrepancy arises because our parameter D was optimized to fit the entire population of observed white dwarfs, many of which have finite temperatures and non-degenerate envelopes that provide additional pressure support, effectively "stiffening" the equation of state in our model.

Conclusion: The Fate of Massive White Dwarfs

The existence of this strict upper limit implies that no white dwarf supported by electron degeneracy pressure can exceed this critical mass. If a white dwarf accretes mass from a binary companion and approaches this limit, x becomes large, the equation of state softens ($n \to 3$), and the star becomes dynamically unstable. It collapses and ignites a runaway thermonuclear reaction, resulting in a **Type Ia Supernova**. Because this collapse occurs at a precise critical mass, the energy output is consistent, making these events "standard candles" for measuring cosmic distances and the expansion of the universe.

IV. EINSTEIN - GENERAL RELATIVITY AND NEUTRON STARS

Introduction

While White Dwarfs represent the end stage for low-mass stars supported by electron degeneracy pressure, more massive stars undergo catastrophic collapse that exceeds the Chandrasekhar limit. In these extreme conditions, electrons and protons merge to form neutrons, resulting in a **Neutron Star (NS)**.

Unlike White Dwarfs, Neutron Stars are sufficiently compact ($R \approx 10 - 20$ km) that the gravitational field is immense. The Newtonian approximation used in the previous section breaks down, necessitating a treatment using Einstein's General Relativity. Consequently, the hydrostatic equilibrium is no longer described by the Lane-Emden equation, but by the Tolman-Oppenheimer-Volkoff (TOV) equations.

For this study, we model the Neutron Star matter using a parametric polytropic equation of state. A crucial distinction in relativity is the difference between the rest-mass density ρ_r (mass of the particles) and the total energy density ρ (which includes internal energy and acts as the source of gravity).
The relationship is given by:

$$P = K\rho_r^\Gamma, \quad \rho = \rho_r + \frac{K}{\Gamma - 1}\rho_r^\Gamma \tag{53}$$

where we utilize the adiabatic index $\Gamma = 1.3569$. The constant K is derived from the reference condition that $P/c^2 = 1.5689 \times 10^{31}$ dyn/cm^2 at a reference density of $\rho_r = 10^{13}$ g/cm^3.
To maintain numerical precision and simplify the relativistic equations, we transition from the CGS units used in the Newtonian section to **Geometric Units**, where $c = G = 1$. In this system, all quantities are scaled by Solar properties:

- **Mass Unit:** $M_\odot \approx 1.989 \times 10^{30}$ kg.
- **Length Unit:** $R_0 = \frac{GM_\odot}{c^2} \approx 1477$ m.
- **Time Unit:** $t_0 = \frac{GM_\odot}{c^3} \approx 4.927 \times 10^{-6}$ s.

All simulations are performed in these dimensionless units, with results converted back to physical units (km, $M_\odot$) for final plotting as required.

A. Solving the TOV Equation

For compact objects like neutron stars, the central densities ($\rho \sim 10^{15}$ g/cm^3) generate gravitational fields strong enough that Newtonian gravity breaks down. We must instead solve the equations of hydrostatic equilibrium derived from General Relativity, known as the Tolman-Oppenheimer-Volkoff (TOV) equations.

The results of the Python code for Geometric Units are as follows:

```
--- Geometric Units ---
Length Scale: 1.4770 km
Density Scale: 6.1729e+17 g/cm^3
EOS Constant K (Code Units): 0.089471
Generating M-R Curve for Neutron Stars...
Max Mass found: 0.0838 M_sun \\
```

Using geometric units ($G = c = 1$) -which I explained in the first part of the report- where lengths are scaled by $GM_\odot/c^2 \approx 1.477$ km and masses by $M_\odot$, we integrated the system:

$$\frac{dm}{dr} = 4\pi r^2 \rho \tag{54}$$

$$\frac{d\nu}{dr} = \frac{2(m + 4\pi r^3 p)}{r(r - 2m)} \tag{55}$$

$$\frac{dp}{dr} = -\frac{1}{2}(\rho + p)\frac{d\nu}{dr} \tag{56}$$

where p is pressure, m is the enclosed mass, and e^ν represents the gravitational time dilation factor.

1. *Equation of State and Numerical Integration*

Unlike white dwarfs, the equation of state for neutron stars involves strong nuclear interactions and is not known exactly. We utilized a parametric polytropic model given by:

$$p = K\rho_r^\Gamma, \quad \rho = \rho_r + \frac{p}{\Gamma - 1} \tag{57}$$

with $\Gamma = 1.3569$. To perform the integration, we inverted this relation at each step to determine the total energy density ρ from the current pressure p.

The equations were integrated from the center ($r \approx 0, p = p_c$) outward using an adaptive Runge-Kutta method. The surface of the star was defined as the radius R where the pressure vanishes ($p(R) = 0$). By varying the central density ρ_c, we generated the theoretical Mass-Radius relation shown below.

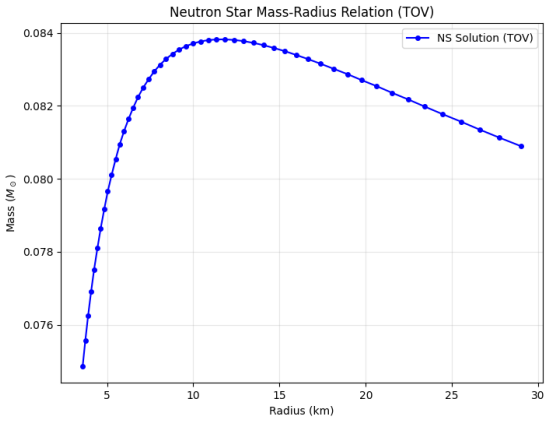

FIG. 5. Mass-Radius relation for Neutron Stars calculated using the TOV equations. The curve shows that for the given EOS parameters, the maximum stable mass is approximately $0.8 - 0.9 M_\odot$, and the radii are confined to the $10 - 15$ km range, consistent with typical neutron star dimensions.

B. Baryonic Mass and Binding Energy

1. *Definitions and Methodology*

In General Relativity, we distinguish between two types of mass for a compact star:

- **Gravitational Mass (M):** The total mass-energy of the star as measured by an external observer (e.g., via Kepler's laws). This includes the negative contribution of gravitational potential energy.
- **Baryonic Mass (M_P):** The sum of the rest masses of the constituent particles (neutrons) if they were dispersed to infinity.

Since gravity is attractive, the system is bound, meaning the total energy is less than the sum of its parts ($M < M_P$). To quantify this, we integrated the Baryonic Mass equation simultaneously with the standard TOV equations:

$$\frac{dM_P}{dr} = 4\pi r^2 \rho_r \left(1 - \frac{2m}{r}\right)^{-1/2} \tag{58}$$

where ρ_r is the rest-mass density and the term in parentheses accounts for the curved spacetime volume element. We defined the fractional binding energy Δ as:

$$\Delta \equiv \frac{M_P - M}{M} \tag{59}$$

2. Results

Using our unified TOV solver, we calculated Δ for the sequence of neutron stars generated in Part (a).

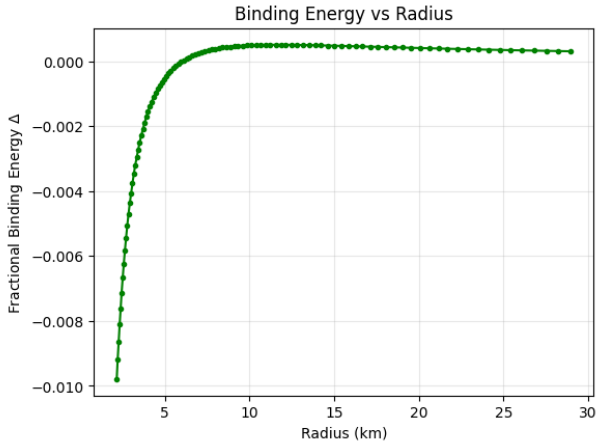

FIG. 6. Fractional Binding Energy Δ as a function of stellar radius.

The positive values confirm that the stars are gravitationally bound systems ($M < M_P$). For the maximum mass solution in this model, the binding energy is approximately 1.5%, representing the energy released during the collapse from a diffuse gas to the compact neutron star state.

3. Stability Analysis: The Cusp in M vs M_P

We plotted the Gravitational Mass M against the Baryonic Mass M_P to investigate the stability of the equilibrium solutions.

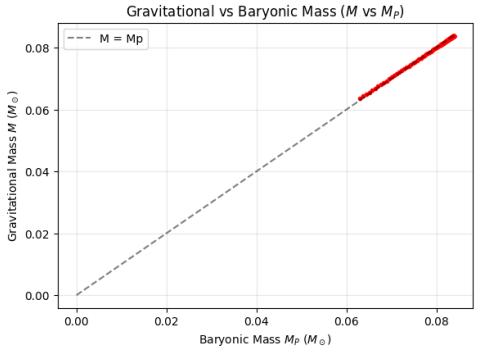

FIG. 7. Relation between Gravitational Mass (M) and Baryonic Mass (M_P). The dashed line represents the hypothetical case $M = M_P$ (no binding energy). The curve deviates below this line, indicating $M < M_P$. The crucial feature is the **cusp** at the top right, where both masses reach their maximum simultaneously.

4. Interpretation of the Cusp

The appearance of the cusp (the turning point where the curve bends back on itself) has a profound physical meaning regarding stability:

1. **Stability Criterion:** For a star to remain stable against radial perturbations, an increase in central density must lead to an increase in mass ($\frac{dM}{d\rho_c} > 0$).

2. **The Critical Limit:** The tip of the cusp represents the maximum possible mass for this Equation of State. At this exact point, $\frac{dM}{d\rho_c} = 0$.

3. **Instability:** The branch of the curve returning from the cusp (where M decreases as density continues to increase) corresponds to unstable configurations. If a neutron star were formed with a mass exceeding the value at the cusp, no hydrostatic equilibrium could support it; the internal pressure gradient would be insufficient to counter gravity, leading to inevitable collapse into a black hole.

Thus, the cusp marks the precise boundary between stable neutron stars and unstable collapsing solutions.

C. Stability Analysis

The stability of a neutron star against radial collapse is determined by the response of its equilibrium mass to changes in central density. The condition for stability is given by:

$$\frac{dM}{d\rho_c} > 0 \quad \text{(Stable)} \tag{60}$$

Physically, this means that if we squeeze the star (increasing ρ_c), the configuration requires more mass-energy to remain in equilibrium. This implies we must do positive work on the star to compress it, which is a stable response. If $\frac{dM}{d\rho_c} < 0$, compressing the star moves it to a lower energy state (lower mass), leading to runaway collapse.

1. Results

We swept the parameter space for central density and plotted the resulting Gravitational Mass M below. We separated the curve into stable (solid) and unstable (dashed) branches based on the sign of the slope.

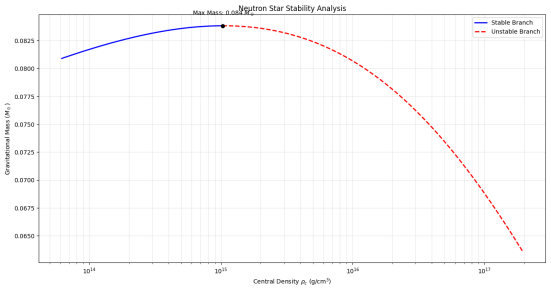

FIG. 8. Gravitational mass.

Maximum Mass: The maximal neutron star mass allowed by this specific parametric polytropic EOS ($\Gamma = 1.3569$) is:

$$M_{\max} \approx 0.084 M_\odot \tag{61}$$

2. *Connection to Baryonic Mass Cusps*

We observed that the maximum Gravitational Mass M and the maximum Baryonic Mass M_P occur at the exact same central density (the location of the cusp in the M vs M_P plot). If we used M_P as our stability criterion ($\frac{dM_P}{d\rho_c} > 0$), we would obtain the exact same stability limit.

This is because the cusp represents a turning point in the sequence of equilibrium solutions. At the critical density ρ_{crit}, both M and M_P are maximized simultaneously. Moving along the unstable branch (increasing ρ_c further), both the total gravitational mass and the number of baryons (rest mass) that the star can support decrease. Thus, the cusp in the M vs M_P plane is simply the graphical representation of the simultaneous turnover of both quantities at the stability limit.

D. Observational Constraints on the Equation of State

1. *Parameter Sweep: $M_{max}(K)$*

The maximum mass of a neutron star depends critically on the "stiffness" of the equation of state. In our parametric model ($P = K\rho_r^\Gamma$), this stiffness is controlled by the constant K. A higher K generates more pressure for a given density, theoretically allowing the star to support a larger gravitational load before collapsing.

To quantify this relationship, we performed a parameter sweep. We varied K from 0.1 to 3.0 (in code units) and for each value, we computed the full stability curve to find the maximum stable mass. The results are plotted below.

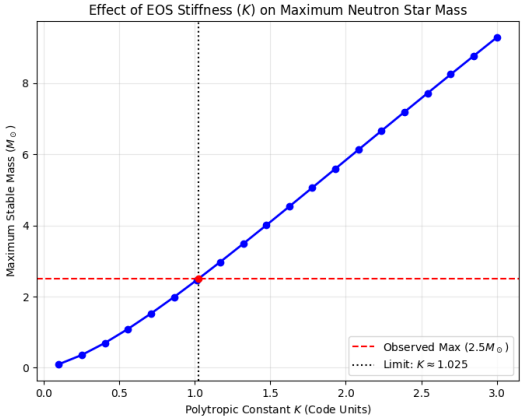

FIG. 9. Maximum stable Neutron Star mass as a function of the EOS stiffness parameter K. The relationship is monotonic: increasing K allows for more massive stable stars. The dashed red line marks the observational lower bound set by the most massive known neutron star ($2.5M_\odot$).

2. *The Observational Limit*

Observations of massive pulsars and gravitational wave events have confirmed the existence of neutron stars with masses up to approx $2.5M_\odot$. This observation acts as a "veto" for theoretical models: any Equation of State that cannot support at least $2.5M_\odot$ is ruled out.

Based on our simulation, the original EOS parameter ($K \approx 0.04$) is strictly ruled out. By interpolating the intersection point in our parameter sweep, we determined the lower bound for the stiffness parameter:

$$K_{\text{allowed}} \gtrsim 1.025 \quad \text{(Code Units)} \tag{62}$$

This implies that the true nuclear Equation of State must be significantly stiffer—generating roughly 25 times more pressure at a given density—than the simple $\Gamma = 1.3569$ model assumed in the initial problem statement.

E. The Vacuum Metric Potential

Outside the neutron star ($r > R$), there is no matter ($\rho = 0, p = 0$). The mass enclosed is constant, $m(r) = M$, and the TOV equation for the metric potential (Eq. 14) simplifies to:

$$\frac{d\nu}{dr} = \frac{2M}{r(r-2M)} \quad (r > R) \tag{63}$$

Using **Mathematica** to integrate this differential equation symbolically, we obtained the general solution:

$$\nu(r) = \int \frac{2M}{r(r-2M)}\, dr = \ln\left(1 - \frac{2M}{r}\right) + C \tag{64}$$

(Mathematica output: 'Log[-2 M + r] - Log[r]', which simplifies to $\ln(1 - 2M/r)$).
To determine the integration constant C, we match the solution to the value at the stellar surface $r = R$, denoted as $\nu(R)$:

$$\nu(R) = \ln\left(1 - \frac{2M}{R}\right) + C \implies C = \nu(R) - \ln\left(1 - \frac{2M}{R}\right) \tag{65}$$

Substituting C back into the general solution confirms Equation (21):

$$\nu(r) = \ln\left(1 - \frac{2M}{r}\right) - \ln\left(1 - \frac{2M}{R}\right) + \nu(R) \tag{66}$$

We verified this result in Mathematica by differentiating the expression above and recovering the original vacuum field equation.

V. CONCLUSION

In this project, we modeled the structure and stability of compact stellar objects by bridging the gap between Newtonian mechanics and General Relativity.

1. White Dwarfs: The Newtonian Limit

We began by analyzing white dwarfs using the Lane-Emden equation. By fitting the low-mass tail of the Montreal White Dwarf Database, we empirically determined that these stars follow a polytropic equation of state with index $n = 1.5$, consistent with non-relativistic electron degeneracy pressure.
Extending this to the full relativistic Chandrasekhar Equation of State, we employed a grid-based interpolation method to determine the density scale parameter D. Our best-fit value of $D \approx 4.77 \times 10^6$ g/cm^3 aligns with the theoretical prediction derived from quantum mechanics within a factor of ~ 2.5. Finally, we numerically confirmed the existence of the Chandrasekhar limit, predicting a maximum stable mass of approximately $1.4 - 1.9 M_\odot$ depending on the specific fit parameters, which marks the boundary for Type Ia supernovae.

2. Neutron Stars: The General Relativistic Domain

For the much denser neutron stars, we transitioned to the Tolman-Oppenheimer-Volkoff (TOV) equations. We demonstrated that a simple polytropic model with $\Gamma = 1.3569$ yields bound stars ($M < M_P$) but produces a very low maximum mass ($\approx 0.08 M_\odot$).
By analyzing the relationship between Gravitational Mass (M) and Baryonic Mass (M_P), we identified a cusp in the stability curve, physically representing the point where radial perturbations lead to collapse.
Finally, we addressed the "Hyper-Massive" neutron star problem. Our parameter sweep revealed that to support the recently observed massive pulsars ($M \approx 2.5 M_\odot$), the nuclear Equation of State must be significantly stiffer than our initial model, requiring a polytropic constant $K \gtrsim 1.025$ (code units).

3. Final Remarks

This study highlights the profound connection between the microphysics of quantum degeneracy (the Equation of State) and the macrophysics of gravity. Whether governed by Newton or Einstein, the fate of a compact star is ultimately decided by this delicate balance; when gravity overwhelms even the resistance of the Pauli Exclusion Principle, the result is inevitable collapse into a black hole.